Journal of Physics B: Atomic, Molecular and Optical Physics

Electron transfer and decay processes of highly charged iodine ions

To cite this article: Hiroyuki A Sakaue *et al* 2004 *J. Phys. B: At. Mol. Opt. Phys.* **37** 403

J. Phys. B: At. Mol. Opt. Phys. **37** (2004) 403–415 PII: S0953-4075(04)68693-7

Electron transfer and decay processes of highly charged iodine ions

Hiroyuki A Sakaue, Atsunori Danjo[1], Kazumoto Hosaka[2], Daiji Kato, Masahiro Kimura[3], Atsushi Matsumoto[4], Nobuyuki Nakamura[5], Shunsuke Ohtani[5], Makoto Sakurai[6], Hiroyuki Tawara[7], Ichihiro Yamada and Masuhiro Yoshino[8]

National Institute for Fusion Science, Toki 509-5292, Japan

Received 9 September 2003
Published 17 December 2003
Online at stacks.iop.org/JPhysB/37/403 (DOI: 10.1088/0953-4075/37/2/008)

Abstract

In the present experimental work we have investigated multi-electron transfer processes in I^{q+} ($q = 10$, 15, 20 and 25) + Ne, Ar, Kr and Xe collisions at $1.5q$ keV energy. Using the coincidence technique between charge-selected projectile and recoil ions, the branching ratios between Auger and radiative decay channels have been measured in decay processes of multiply excited states formed by multi-electron transfer collisions. By combining these ratios with the measured absolute cross sections for total and single electron transfer processes, the partial cross sections for various charge changing processes have been determined. It has been shown that, in all the multi-electron transfer processes investigated, the Auger decays are far dominant over the radiative decay processes and the branching ratios are clearly characterized by the average principal quantum number $\langle n \rangle$ of the initial excited states of projectile ions, estimated from the extended classical-over-barrier-model (ECBM). We could express the branching ratios in high Rydberg states formed in multi-electron transfer processes by using the decay probability of one Auger electron emission.

[1] Present address: Department of Environmental Science, Niigata University, Niigata 950-2181, Japan.
[2] Present address: National Physical Laboratory, Teddington TW11 0LW, UK.
[3] Present address: Kochi University of Technology, Kochi 782-8502, Japan.
[4] Present address: Hiroshima Institute of Technology, Hiroshima 731-5193, Japan.
[5] Present address: The University of Electro-Communications, Chofu 182-8585, Japan.
[6] Present address: Department of Physics, Kobe University, Kobe 657-8501, Japan.
[7] Present address: Max Planck Institute for Nuclear Physics, Saupfercheckweg 1, D-69117 Heidelberg, Germany.
[8] Present address: Shibaura Institute of Technology, Saitama 337-8570, Japan.

1. Introduction

To date, multiple electron capture processes in collisions of highly charged ions (HCIs) A^{q+} with atoms B have been widely studied (Barat and Roncin 1992). The electron capture cross sections in HCI–atom collisions have been understood reasonably well through the classical over-barrier model (Ryufuku and Sasaki 1980, Mann *et al* 1981, Mann 1986, Barany and Hvelplund 1987). The energy deposition model has also been used successfully to apply the observed Auger decay processes and multiple ionization processes (Russek 1963, Cock 1979, Müller *et al* 1983). Recent activities on those studies are reviewed by Cederquist *et al* (1999). Such collisions generally produce multiply excited states $A^{(q-j)+**\cdots}(n, n', \ldots)$, which in turn are stabilized through emissions of electron(s) and photon(s):

$$\begin{aligned} A^{q+} + B &\rightarrow A^{(q-j)+**\cdots}(n, n', \ldots) + B^{j+} \\ &\rightarrow A^{(q-i)+} + B^{j+} + (j-i)e^{-} + h\nu + h\nu' + \cdots \end{aligned}$$

where q represents the charge of the incident projectile ion, j the number of the electrons initially transferred into the ion from target atom during the collision, i the final charge change of the incident ion after stabilization and $(n, n', \ldots)$ shows the principal quantum numbers of the electron transferred states. Since various combinations of j and i are possible, multiple electron capture processes are so complicated that systematic investigations are needed for a detailed understanding. Various Auger and radiative decay pathways following multiple electron capture were studied by de Nijs *et al* (1996). On the other hand, in our previous work (Yamada *et al* 1995, Nakamura *et al* 1995), the partial electron capture cross sections $\sigma^{j}_{q,q-i}$ have been determined for I^{q+} + Ne, Ar, Kr, and Xe ($q = 10$ and 15) collisions through coincidence measurements in the charge state distribution of projectile and target recoil ions. In those studies, it was found that the multiply excited states produced in collisions tend to be stabilized by emission of many low-energy electrons rather than ejection of a few high-energy electrons.

In this study, the previous work is extended to still higher q to investigate the stabilization processes of higher excited states. In general, the electron transferred levels become higher as the charge of the incident ion increases. We discuss the branching ratios of decay processes as a function of the average principal quantum number '$\langle n \rangle$' of the electron transferred levels. Furthermore, the projectile ion charge dependence of the electron transfer cross sections $\sigma^{j}_{q} = \sum_i \sigma^{j}_{q,q-i}$ and the total electron transfer cross sections $\sigma_q = \sum_j \sigma^{j}_{q}$ are also discussed by comparison with the extended classical over-barrier model (ECBM) (Niehaus 1986).

In this paper the term 'transfer' refers to processes where electrons are removed from target atoms to the projectile ions during collisions, whereas the term 'capture' refers to processes where electrons remain bound to the projectile ions after stabilization.

2. Experiments

The present experimental apparatus and method were the same as those used in the previous work (Nakamura *et al* 1995). Two different types of measurements were made using the electron beam ion source called NICE (Kaneko *et al* 1981).

First, absolute total (σ_q) and one-electron capture cross sections ($\sigma_{q,q-1}$) were measured by the initial growth-rate method combined with the energy retardation technique. Second, the charge state distributions of product ions were measured in coincidence with those of recoil ions. Figure 1 shows a typical result of the coincidence measurement for I^{20+} + Xe collisions, where the transfer processes of up to eight electrons were clearly observed. We can also see a peak ($j = 1, i = 2$) in this spectrum which is due to double collisions. The fraction of the

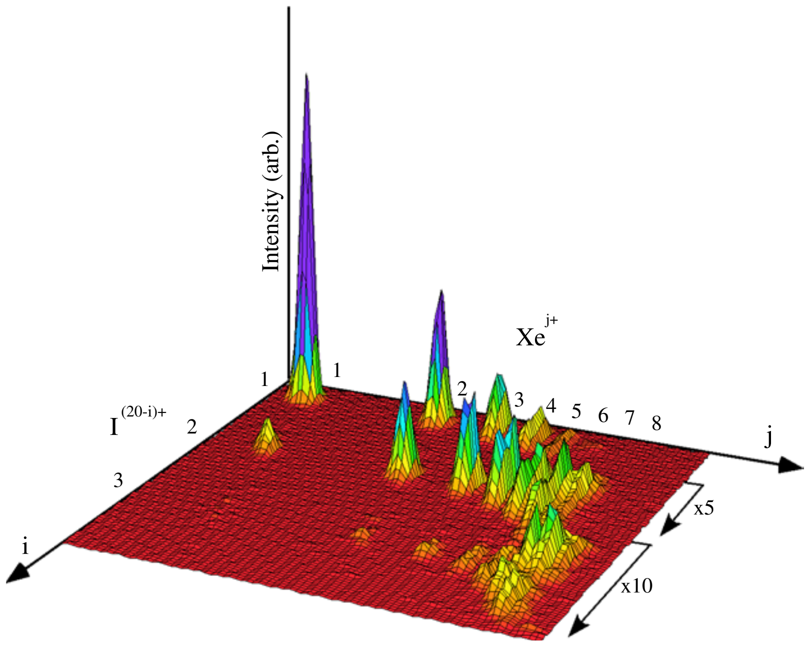

Figure 1. Typical coincidence spectrum for the charge state distributions between the product ions and the recoil ions in I^{20+} + Xe collisions.

(This figure is in colour only in the electronic version)

double collision was estimated to be a few per cent. By combining the experimental results of the absolute one-electron capture cross sections with the coincidence measurements between the charge-state-selected projectile and recoil ions, we have deduced the absolute values for σ_q^j and $\sigma_{q,q-i}^j$ in I^{20+} + Ar and Xe collisions. The j-electron transfer cross sections have also been determined for $q = 25$.

The collision energies were fixed at $1.5q$ keV for all of the measurements. Most of the experimental errors in the present cross section measurements originated from determination of the target thickness. The target gas cell was connected to a gas reservoir through a capillary tube. In our previous experiment, the target density had been estimated by using values for the calculated conductances of the capillary tube and the cell apertures, and also by the absolute pressure in the target gas reservoir, which was measured with a capacitance manometer. In the present experiment, the effective conductance was measured directly through the measurement of time constant of gas pressure decrease in the target gas reservoir. From our measurement of the effective conductance, we could estimate the target density with higher precision. Total experimental uncertainty for the absolute values of each cross section was estimated to be ±13–19%. Our previously measured data (Yamada *et al* 1995, Nakamura *et al* 1995) of the cross sections were also corrected.

3. Result and discussion

In this paper, we consider the following multiple electron capture processes in highly charged iodine ion ($q = 10$, 15, 20 and 25) collisions with the rare gas atom (Ne, Ar, Kr and Xe):

$$I^{q+} + B \rightarrow I^{(q-i)+} + B^{j+} + (j - i)e^- + \sum h\nu + Q. \tag{1}$$

Here the cross section can be described as $\sigma^{j}_{q,q-i}$, Q is the translational energy gain in the collision, and $\sum$ represents the cascade photon emissions.

It is convenient to discuss the electron capture processes by dividing into the following two steps.

(I) j-electron transfer process:

$$\mathrm{I}^{q+} + \mathrm{B} \to \mathrm{I}^{(q-j)+**\cdots}(n, n', \ldots) + \mathrm{B}^{j+} + Q$$

where $n, n', \ldots$ are the principal quantum numbers of the electronic states produced in this process. The cross section for the process is given as σ^{j}_{q}.

(II) Decay process of the excited product ion:

$$\mathrm{I}^{(q-j)+**\cdots}(n, n', \ldots) \to \mathrm{I}^{(q-i)+} + (j-i)\mathrm{e}^{-} + \sum h\nu.$$

First we show the measurements for the total σ_q and the j-electron transfer cross sections σ^{j}_{q} and partial cross sections $\sigma^{j}_{q,q-i}$ in section 3.1, and then discuss the branching ratios of the above decay processes (II) in multiply excited product ions in section 3.2.

3.1. Measurements of cross sections

The cross sections have been measured for total (σ_q) and j-electron (σ^{j}_{q}) transfer processes in I^{q+} + B collisions ($q = 10$, 15, 20 and 25, B = Ar and Xe). We assume that the recoil ion charge state j is equal to the number of transferred electrons to the projectile ions: that is, we consider the direct ionization of target atoms and the autoionization of target ions to be negligibly small at the present collision energies.

Figures 2(a) and (b) show the charge dependence of the absolute total σ_q and j-electron transfer cross sections σ^{j}_{q} ($j = 1$–3) for Ar and Xe targets, respectively. The calculated values based upon ECBM are also shown. From our experimental data we found that, as the incident ion charge increases, the observed total electron transfer cross sections σ_q increase roughly proportional to the charge q for both Ar and Xe targets. Generally, the cross sections are larger for the Xe target than for the Ar. This is because the binding energy of electrons to be transferred is smaller in Xe than in Ar, as discussed in our previous paper (Kimura *et al* 1995). Our experimental values of the total electron transfer cross sections agree with the ECBM calculations within the experimental uncertainties. It has been found that the j-electron transfer cross sections σ^{j}_{q} ($j = 1$–3) also increase as the incident ion charge increases. For the Xe target, the experimental values of j-electron transfer cross sections agree well with the ECBM calculations. However, for the Ar target, the observed one-electron transfer cross sections σ^{1}_{q} are obviously larger than ECBM calculations. In addition, the observed two- and three-electron transfer cross sections (σ^{2}_{q} and σ^{3}_{q}) have been found to level off for higher projectile charge and to be small in comparison with the ECBM values. This tendency had been observed in our previous experiment (Nakamura *et al* 1995) for I^{q+} + Ne collisions and also in Ar^{q+} + Ar collisions (Ali *et al* 1994).

In figures 3(a)–(c) we show the absolute partial cross sections for i-electron capture into projectile ions after j-electron transfer from target ($\sigma^{j}_{q,q-i}$) in collisions of I^{q+} ($q = 10$, 15 and 20) with Ar and Xe targets, respectively, and list them in table 1. The following features should be pointed out in these observed data:

(1) The cross sections for one-electron capture ($i = 1$) after j-electron transfer ($\sigma^{j}_{q,q-1}$) decrease almost monotonically as the number of transferred electron increases.

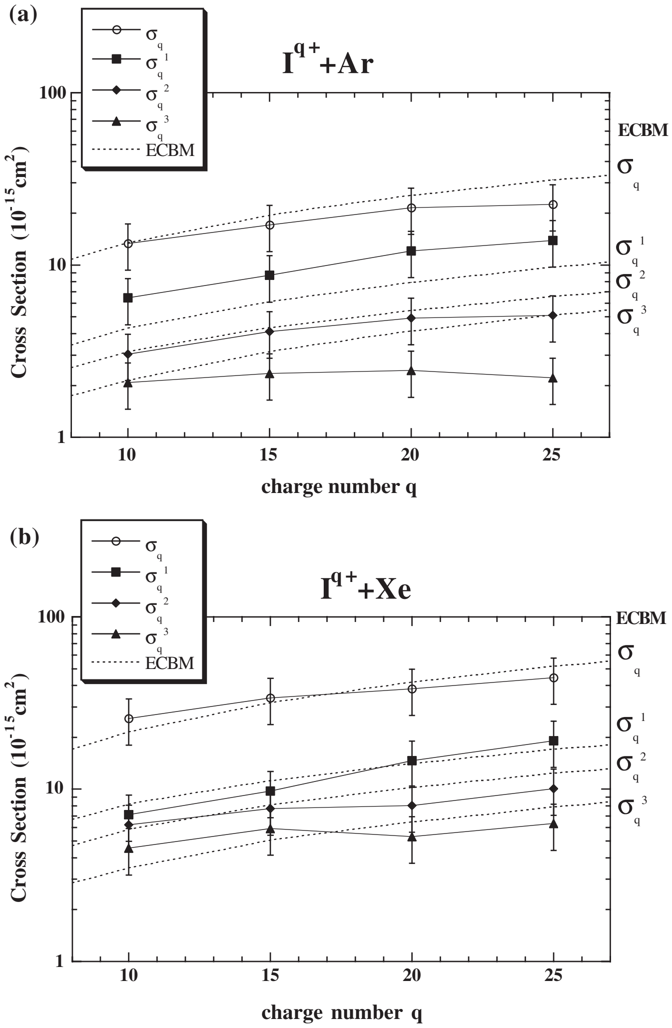

Figure 2. Absolute total σ_q and j-electron transfer cross sections σ_q^j in (a) I^{q+} + Ar and (b) I^{q+} + Xe ($q = 10$–25) collisions. The calculated values of ECBM are represented by the dotted curves.

(2) For both Ar and Xe targets, as the number of transferred electrons increases, the cross sections for multi-electron capture ($\sigma^j_{q,q-2}$ and $\sigma^j_{q,q-3}$) increase first and then reach a maximum at a certain number of the transferred electrons except for $\sigma^j_{20,18}$ and finally decrease. For example, two-electron capture cross sections $\sigma^j_{10,8}$ become maximum at $j = 4$ in I^{10+} + Xe collisions. This maximum peak shifts toward a large number of j as charge q increases: that is, two-electron capture cross sections of $q = 10$, 15 and 20 ($\sigma^j_{10,8}$, $\sigma^j_{15,13}$ and $\sigma^j_{20,18}$) for Xe targets have maxima at $j = 4$–6, respectively. The maximum j value for the Xe target in the respective i-electron capture process is seen to be larger than that for the Ar.

(3) The two-electron capture cross sections ($\sigma^j_{q,q-2}$) become larger than the one-electron capture cross sections ($\sigma^j_{q,q-1}$) at higher j. Similarly the three-electron capture cross

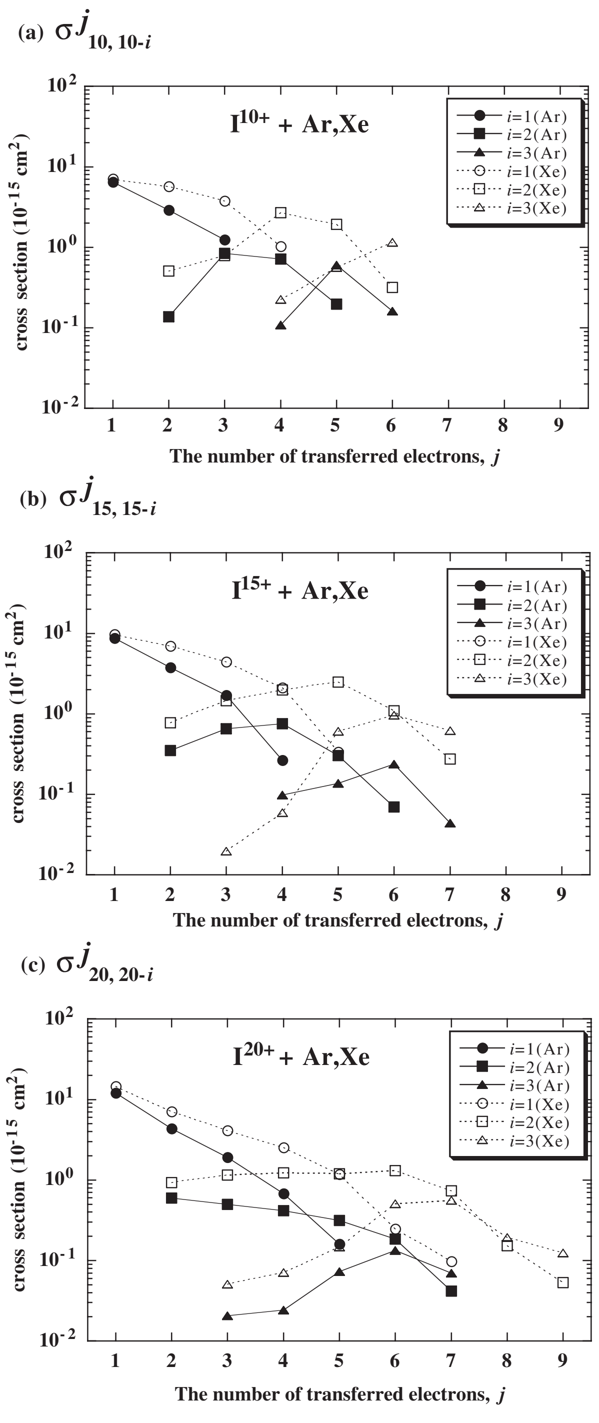

Figure 3. The j dependence of the absolute partial cross sections $\sigma^{j}_{q,q-i}$ in I^{q+} + Ar and Xe collisions. (a)–(c) correspond to $q = 10$, 15 and 20, respectively. The solid and dotted curves are drawn to guide the eye for the Ar and Xe targets, respectively.

Table 1. The absolute partial cross sections $\sigma^{j}_{q,q-i}$ $(10^{-15}\ \mathrm{cm}^2)$. Total experimental uncertainties for the absolute values of each cross section were estimated to be ±13–19%.

			j								
			1	2	3	4	5	6	7	8	9
$q = 10$											
Ar	i	1	6.4	2.9	1.2						
		2		0.14	0.84	0.71	0.20				
		3				0.19	0.60	0.16			
Xe	i	1	7.2	5.7	3.8	1.0					
		2		0.51	0.80	2.7	1.9	0.32			
		3				0.23	0.56	1.2			
$q = 15$											
Ar	i	1	8.7	3.8	1.7	0.26					
		2		0.35	0.65	0.75	0.30	0.070			
		3				0.098	0.14	0.24	0.044		
Xe	i	1	9.7	6.9	4.4	2.1	0.33				
		2		0.78	1.5	2.0	2.5	1.1	0.27		
		3			0.020	0.059	0.61	0.96	0.62		
$q = 20$											
Ar	i	1	12	4.3	1.9	0.68	0.16				
		2		0.60	0.50	0.41	0.31	0.18	0.042		
		3			0.021	0.024	0.073	0.13	0.070		
Xe	i	1	15	7.1	4.1	2.5	1.2	0.25	0.097		
		2		0.93	1.2	1.2	1.2	1.3	0.74	0.15	0.054
		3			0.051	0.071	0.15	0.51	0.56	0.19	0.12

sections ($\sigma^{j}_{q,q-3}$) dominate over the two-electron capture cross sections in a much higher j region. For a large number of electron transfer processes, the present analysis has suggested that more electrons transferred into high excited states of the projectile ions are emitted through Auger decay processes.

3.2. Branching ratios of decay processes

In this section, we consider the decay processes (II) of multiply excited ions produced by multi-electron transfer processes. We have determined the branching ratios in the decay of multiply excited ions from the coincidence measurement of the scattered and recoil ions. The branching ratios $P(j, j-i)$ in the decay of multiply excited ions by emission of $(j-i)$ electrons after j-electron transfer is defined by

$$P(j, j-i) = \frac{\sigma^{j}_{q,q-i}}{\sum_i \sigma^{j}_{q,q-i}} = \frac{\sigma^{j}_{q,q-i}}{\sigma^{j}_{q}}.$$

The following discussion is based on several assumptions. The first one is that the recoil ion charge state j is equal to the number of electrons initially transferred into projectile ions, similarly to that described in section 3.1. In slow HCI collisions, the electrons are generally transferred to higher excited levels in projectile ions from target atoms as the ion charge increases, because the Coulomb potential energy of the projectile becomes larger and thus the captured levels in the projectile whose energies are resonant with the binding energies of electrons in the target become higher. Moreover, in many electron transfer processes involving target atoms with closed-shell structures such as rare gas atoms, the transferred electrons are expected to originate from the outermost shell of the targets having similar and low binding energy. Therefore the n-values for multi-electron transfer processes are expected to be similar for the present target atoms which have similar ionization energies. We also assume that the Auger decay rates of multiply excited states with high n-values do not depend strongly on the ion charge, but the number of Auger processes depends on the number of the decay channels from the excited states. Since the number of decay channels is related to the degree of the n-value, the probability of the decay process with j-electrons transferred can be expressed by using the following average value $\langle n\rangle$ of all j electrons:

$$\langle n\rangle = \frac{(n_1 + n_2 + \cdots + n_j)}{j}.$$

Here n_j represents the principal quantum number of the jth electron transferred which can be estimated from the ECBM (Niehaus 1986).

Figure 4 shows one of the possible arrangements for the relationship between the branching ratios and the average principal quantum number $\langle n\rangle$. Here, we plot the measured branching ratios as a function of $-1/\langle n\rangle^2$, where $\langle n\rangle$ is the value calculated with the ECBM for each j-electron transfer process. In this figure, all of our experimental data for I^{q+} + B collisions (q = 10, 15 and 20, B = Ne, Ar, Kr and Xe) including the previous data (Yamada *et al* 1995, Nakamura *et al* 1995) are shown. Here we also show the threshold values n_{thre} of the energetically allowed Auger decay processes for the respective branching ratio $P(j, j-i)$, which is calculated as follows.

Since such Auger electrons have positive energy in the process for j-electron transfer followed by i-electron capture where $(j-i)$ electrons are ejected, the following relation should be satisfied:

$$I_P(\mathrm{I}^{(q-i)+} \to \mathrm{I}^{q+}) - I_P(\mathrm{B} \to \mathrm{B}^{j+}) - Q \geqslant 0 \qquad (2)$$

where $I_P(\mathrm{I}^{(q-i)+} \to \mathrm{I}^{q+})$ is the ionization energy required to ionize $\mathrm{I}^{(q-i)+}$ to I^{q+}. From equation (2) the maximum value of energy gain Q_{max} can be determined as

$$Q_{\mathrm{max}} = I_P(\mathrm{I}^{(q-i)+} \to \mathrm{I}^{q+}) - I_P(\mathrm{B} \to \mathrm{B}^{j+}).$$

When the energy gain Q is smaller than Q_{max}, the processes (1) are energetically allowed. We calculated the principal quantum number n_{thre} for the electron transferred levels based upon the ECBM at $Q = Q_{\mathrm{max}}$ in the collision systems investigated: I^{q+} + B (Ne, Ar, Kr and Xe). Calculated n_{thre} values are slightly different for the target atoms with different ionization energies, which are shown by shaded bars in figure 4. Although the solid and dotted curves are drawn to guide the eyes, they show the general dependence of the branching ratios on the $\langle n\rangle$-values. In drawing these curves, we take the following simple principles into account: (1) the $P(j, j-i)$ branching ratio is zero when the average transfer levels $\langle n\rangle$ are lower than the threshold levels n_{thre} and (2) the sum of the branching ratios equals 1.0.

(A) *Doubly excited states*. In the doubly excited states (figure 4(a)), we can place the branching ratio of the radiative decay to be 1.0 when the average transfer levels $\langle n\rangle$ are lower than $n_{\mathrm{thre}} \cong 5.7$ which corresponds to the threshold levels for the $P(2, 1)$ processes. On the other hand, as q becomes higher, the highly charged ions capture electrons into higher excitation levels than the threshold ($n_{\mathrm{thre}} \cong 5.7$), where the Auger decay becomes energetically possible. In these cases, the single Auger decay becomes dominant and the branching ratios show almost constant value. Actually, as shown in our experimental

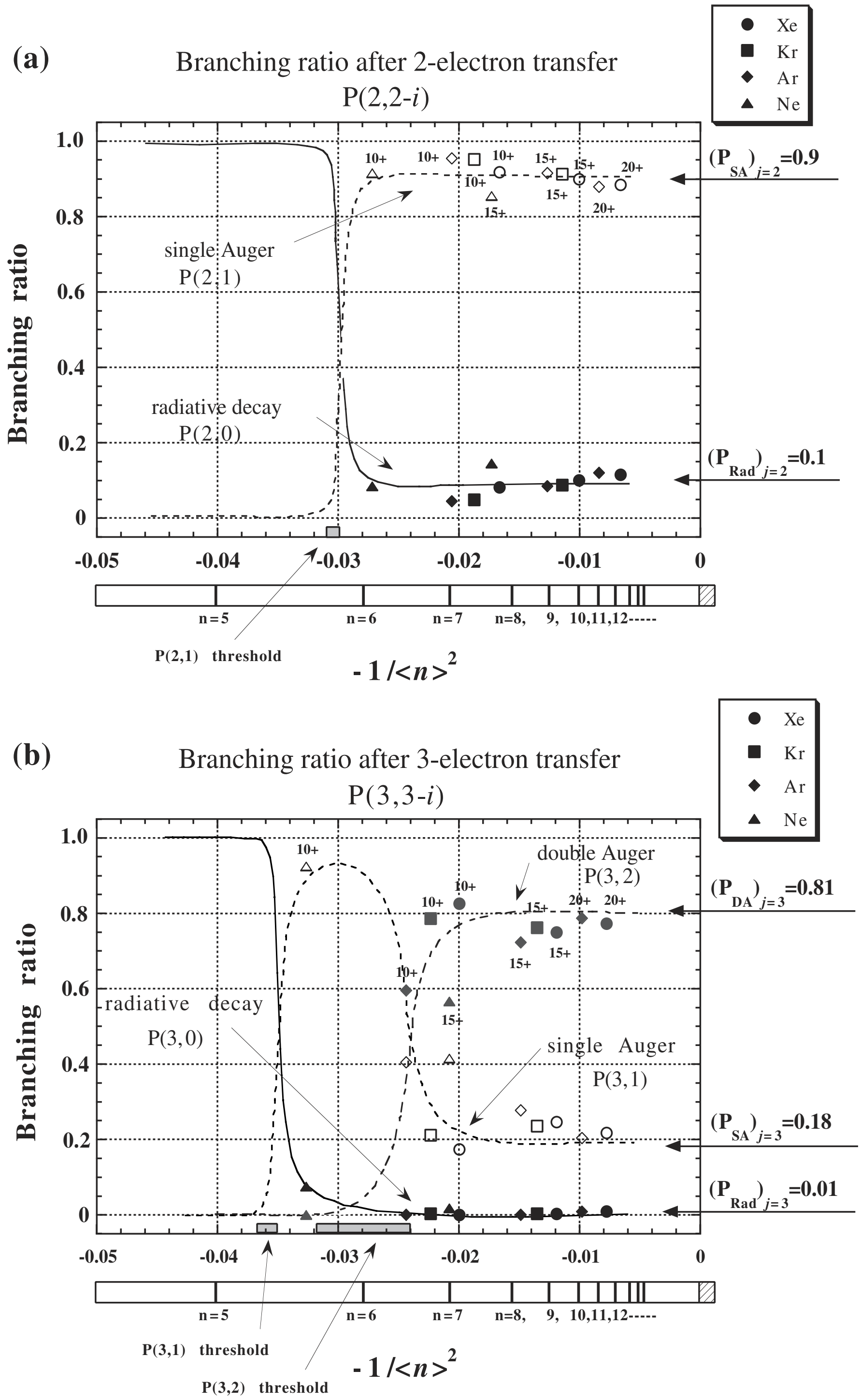

Figure 4. $-1/\langle n\rangle^2$ dependence of the branching ratios $P(j, j-i)$. n is the principal quantum number of the transferring excited levels calculated by ECBM. (a)–(c) correspond to $j = 2$, 3 and 4, respectively.

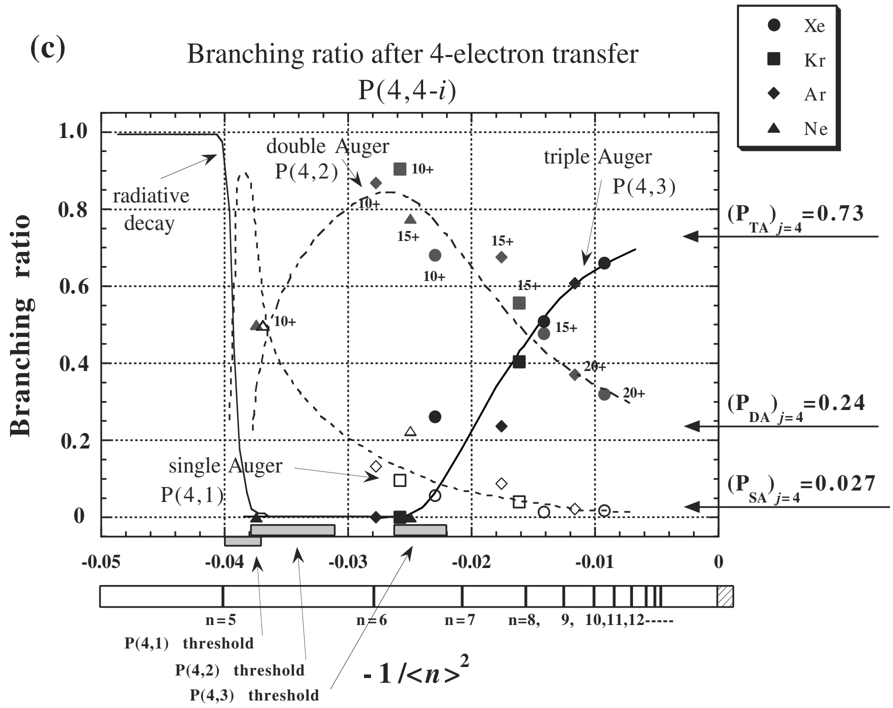

Figure 4. (Continued.)

results with charge state range of $q = 10$–20, the branching ratio $P(2,1)$ has been determined to be 0.9, while the branching ratio of radiative decay $P(2,0)$ is about 0.1, indicating that the radiative decay rate is much smaller than the Auger decay rate. It is interesting to note that, in Xe^{q+} + Xe, He collisions (Cederquist *et al* 1992), the rapid increase of the radiative decay branching ratio $P(2,0)$ was observed in the higher q region where the number of vacancies in the 3d shell of the Xe^{q+} projectile increases. For the present I^{q+} + B collision systems, since there is no 3d-vacancy in I^{q+} projectiles with $q < 26$, no significant increase of $P(2,0)$ has been observed in the present q range investigated ($10 \leqslant q \leqslant 20$). When the ion charge is lower than 28 in Xe^{q+} + Xe, He collisions (Cederquist *et al* 1992), $P(2,0)$ does not show strong dependence on the ion charge but has the value of 0.05–0.1 which is consistent with the present experiment.

(B) *Triply excited states*. In the triply excited states (figure 4(b)), when three electrons are bound to the comparatively deep inner shells ($5.3 \leqslant \langle n\rangle \leqslant 6$) of the ion, the excited states of ions decay dominantly by emitting one electron. However, when the electrons are transferred to levels higher than the $P(3,2)$ threshold level ($n_{\mathrm{thre}} \cong 6$), the single Auger decay processes start to decrease, and instead the double Auger decay processes start to increase gradually. When the three electrons are transferred to higher excited states ($\langle n\rangle \geqslant 8$), the fraction of the double Auger decay reaches up to about 0.8. Finally, all of the branching ratios ($P(3,0)$, $P(3,1)$ and $P(3,2)$) keep roughly constant in the high $\langle n\rangle$ region, where the radiative decay processes almost disappear and the Auger decay processes become dominant. Though the projectile q value is quite different for I^{15+} + Xe and I^{20+} + Ar collisions, the branching ratios are nearly the same as seen in figure 4(b). This is because the transferred levels are almost the same ($\langle n\rangle \cong 10$), which shows that the Auger rates do not depend on the ionic charge q, but on the average principal quantum number $\langle n\rangle$ related to the number of the decay channels.

(C) *Quadruply excited states*. Similarly, in the quadruply excited states (figure 4(c)), the double Auger decay processes increase as the single Auger decay processes decrease at $\langle n\rangle \cong 5.3$ and afterwards become dominant at $\langle n\rangle \cong 6$. The triple Auger decay channel is opened at $\langle n\rangle \cong 6.3$, the threshold for $P(4,3)$. The ratios of double and triple Auger decays are turned inversely near $\langle n\rangle \cong 8$. If the four electrons are transferred into still higher excited states ($\langle n\rangle \geqslant 11$), the triple Auger decay channels become dominant and the $P(4,3)$ approaches to about 0.7.

Through the above arrangements of experimental data, we have summarized the general feature in the decay processes from the multiply excited states produced by many-electron transfer collisions. When electrons are transferred to higher levels than the threshold $\langle n_{\rm thre}\rangle$, the Auger decay dominates rather than the radiative decay. Then as the transferred levels go up to higher $\langle n\rangle$, the Auger decay with more than one-electron emission becomes favourable. Finally, all of the branching ratios for radiative and Auger decay processes take constant values as an asymptotic characteristic with high $\langle n\rangle$.

We will discuss the observed systematic behaviour for the decay processes of highly excited ions with multi-Rydberg electrons. First, we define $R_{\rm Auger}$ as the decay probability with single Auger electron emission and $R_{\rm rad}$ as the radiative decay probability, respectively, from sufficiently high $\langle n\rangle$ levels produced by the multi-electron transfer, where $R_{\rm Auger} + R_{\rm rad} = 1$. For the doubly excited states with $\langle n\rangle$ higher than the threshold level $n_{\rm thre} = 5.7$, the branching ratios $P(2,1)$ and $P(2,0)$ become constant and are 0.9 and 0.1, respectively, as shown in figure 4(a). Therefore, the $R_{\rm Auger}$ corresponds to the asymptotic value of the branching ratio for the single Auger electron decay from the doubly excited state produced by two-electron transfer ($j = 2$) collision: $(P_{\rm SA})_{j=2} = P(2,1)$, and the $R_{\rm rad}$ also corresponds to the branching ratio for the radiative decay: $(P_{\rm rad})_{j=2} = P(2,0)$, and these are determined experimentally as follows:

$$
\begin{aligned}
(P_{\rm SA})_{j=2} &= R_{\rm Auger} = 0.9\\
(P_{\rm rad})_{j=2} &= R_{\rm rad} = 0.1.
\end{aligned}
$$

In three and four-electron transfer collisions, triply and quadruply excited states can be produced, which may decay radiatively and eject two or three electrons. Here, we make assumptions that, for the multiply excited states with asymptotically high $\langle n\rangle$, the successive Auger decay processes are favourable, which take place successively with combination of cascading single Auger processes, whose probabilities are nearly the same because the multi-electrons still remain in high Rydberg states after the first and the succeeding Auger decay processes. On the other hand, we suppose that the multi-Auger decay processes ejecting correlated two or three electrons simultaneously is negligible.

Next, we discuss the decay processes from the triply excited states with high $\langle n\rangle$. There are three possible processes with own branching ratios: (1) the successive double Auger decay: $(P_{\rm DA})_{j=3}$, (2) the combination of single Auger and radiative decay: $(P_{\rm SA})_{j=3}$ and (3) the combination of two pure radiative decays $(P_{\rm rad})_{j=3}$. Based on the above assumptions, the respective branching ratios are expressed as follows:

$$
\begin{aligned}
(P_{\rm DA})_{j=3} &= (R_{\rm Auger})^2,\\
(P_{\rm SA})_{j=3} &= R_{\rm Auger} \times R_{\rm rad} + R_{\rm rad} \times R_{\rm Auger}\\
&= 2 \times R_{\rm Auger} \times R_{\rm rad} = 2 \times R_{\rm Auger} \times (1 - R_{\rm Auger}),\\
(P_{\rm rad})_{j=3} &= (R_{\rm rad})^2 = (1 - R_{\rm Auger})^2.
\end{aligned}
$$

As the asymptotic value of R_{Auger} has been found to be 0.9 from our experiment, the above branching rations are calculated to be $(P_{\text{DA}})_{j=3} = 0.81$, $(P_{\text{SA}})_{j=3} = 0.18$ and $(P_{\text{rad}})_{j=3} = 0.01$. These values are shown in figure 4(b) with horizontal arrows. The calculated branching ratios are in good agreement with the asymptotic values in the observations, as seen in figure 4(b), for three-electron transfer processes.

By extending similar discussion to the decay processes from the quadruply excited states, the branching ratios of the stabilization probabilities with the triple, double, single Auger and pure radiative decay ($(P_{\text{TA}})_{j=4}$, $(P_{\text{DA}})_{j=4}$, $(P_{\text{SA}})_{j=4}$ and $(P_{\text{rad}})_{j=4}$) can be described as follows:

$$
\begin{aligned}
&(P_{\text{TA}})_{j=4} = (R_{\text{Auger}})^3, \\
&(P_{\text{DA}})_{j=4} = 3 \times (R_{\text{Auger}})^2 \times R_{\text{rad}} = 3 \times (R_{\text{Auger}})^2 \times (1 - R_{\text{Auger}}), \\
&(P_{\text{SA}})_{j=4} = 3 \times R_{\text{Auger}} \times (R_{\text{rad}})^2 = 3 \times R_{\text{Auger}} \times (1 - R_{\text{Auger}})^2, \\
&(P_{\text{rad}})_{j=4} = (R_{\text{rad}})^3 = (1 - R_{\text{Auger}})^3.
\end{aligned}
$$

The calculated values are $(P_{\text{TA}})_{j=4} = 0.73$, $(P_{\text{DA}})_{j=4} = 0.24$, $(P_{\text{SA}})_{j=4} = 0.027$ and $(P_{\text{rad}})_{j=4} = 0.001$, respectively. These values are shown in figure 4(c) and again found to reproduce the observed values.

In summary, we have speculated about the decay processes from the highly excited ions with multi-Rydberg electrons. Asymptotic characteristics of the branching ratios for the related decay modes are described as a combination of successive Auger processes, and well reproduced in terms of the probability determined in the observation of decay processes from the doubly excited ions with asymptotically high Rydberg electrons.

4. Conclusions

We have experimentally determined the absolute total electron transfer cross section σ_q, partial cross sections σ_q^j and $\sigma_{q,q-i}^j$ and the branching ratios $P(j, j-i)$ in low energy I^{q+} ($q = 10$, 15, 20 and 25) + Ar and Xe collisions.

The present results of total electron transfer cross sections σ_q and j-electron transfer cross sections σ_q^j of Xe target agree well with the predictions of the ECBM within the experimental errors.

The present observation of branching ratios suggests that the Auger decay processes after multiple electron transfer are characterized by the principal quantum number n of the transferred level and are nearly independent of the projectile ion charge q for $q = 10$–20 range. From our analysis for the asymptotic behaviour in the branching ratios, the multiple-Auger decay process for multiply highly excited states can be treated as a succession of the single Auger process. We have found that the branching ratios in high Rydberg states formed in multi-electron transfer processes can be expressed in terms of the decay probability (R_{Auger}) for one Auger electron emission.

Acknowledgment

This work was performed as a part of the Guest Research Programme at the National Institute for Fusion Science.

References

Ali R, Cocke C L, Raphaelian M L A and Stockli M 1994 *Phys. Rev.* A **49** 3586
Barany A and Hvelplund P 1987 *Nucl. Instrum. Methods* B **23** 40

Barat M and Roncin P 1992 *J. Phys. B: At. Mol. Opt. Phys.* **25** 2205
Cederquist H *et al* 1992 *Phys. Rev.* A **46** 2592
Cederquist H, Fardi A, Haghighat K, Langereis A, Schmidt H T and Schwartz S H 1999 *Phys. Scr.* T **80** 46
Cock C L 1979 *Phys. Rev.* A **20** 749
de Nijs G, Hoekstra R and Morgenstern R 1996 *J. Phys. B: At. Mol. Opt. Phys.* **29** 6143
Kaneko Y, Iwai T, Ohtani S, Okuno K, Kobayashi N, Tsurubuchi S, Kimura M and Tawara H 1981 *J. Phys. B: At. Mol. Phys.* **14** 881
Kimura M *et al* 1995 *J. Phys. B: At. Mol. Opt. Phys.* **28** L643
Mann R 1986 *Z. Phys.* D **3** 85
Mann R, Folkmann F and Beyer H K 1981 *J. Phys. B: At. Mol. Phys.* **14** 1161
Müller A, Groh W and Salzborn E 1983 *Phys. Rev. Lett.* **51** 107
Nakamura N *et al* 1995 *J. Phys. B: At. Mol. Opt. Phys.* **28** 2959
Niehaus A 1986 *J. Phys. B: At. Mol. Phys.* **19** 2925
Russek A 1963 *Phys. Rev.* **132** 246
Ryufuku H and Sasaki K 1980 *Phys. Rev.* A **21** 745
Yamada I *et al* 1995 *J. Phys. B: At. Mol. Opt. Phys.* **28** L9